mTOR inhibition in primary neurons and the developing brain represses transcription of cholesterol biosynthesis genes and alters cholesterol levels

Martin Schüle[1,5], Tamer Butto[1], Sri Dewi[1], Susanne Strand[2], Susanne Gerber[1], Kristina Endres[3], Susann Schweiger[1,4,5], Jennifer Winter[1,4,5*]

[1] Institute of Human Genetics, University Medical Center Mainz Johannes Gutenberg-University, 55131 Mainz, Germany
[2] First Department of Internal Medicine, University Medical Center Mainz, 55131 Mainz, Germany
[3] Department of Psychiatry and Psychotherapy, University Medical Center Johannes Gutenberg-University, 55131 Mainz, Germany.
[4] German Resilience Centre, University Medical Center Mainz, 55131 Mainz, Germany
[5] Focus Program of Translational Neurosciences, University Medical Center Mainz, 55131 Mainz, Germany

[*]Correspondence: PD Dr. Jennifer Winter, Institute of Human Genetics, University Medical Center Mainz, Langenbeckstr. 1, 55131 Mainz, Germany, jewinter@uni-mainz.de

Abstract

Dysregulated mammalian target of rapamycin (mTOR) activity is associated with various neurodevelopmental disorders ranging from idiopathic autism spectrum disorders to monogenic syndromes as for example Tuberous sclerosis complex. Thus, maintaining mTOR activity levels in a physiological range is essential for brain development and functioning. Upon activation, mTOR regulates a variety of cellular processes such as cell growth, autophagy and metabolism. On a molecular level, however, the consequences of mTOR activation are not well understood, especially in the brain. Thus, while it was shown that in cells outside the central nervous system mTORC1 activity is necessary for activating gene transcription of different metabolic pathways this mechanism is ill defined in the brain.

By combining mTORC1 inhibition with RNA-sequencing we identified numerous genes of the sterol/cholesterol biosynthesis pathway to be downstream targets of mTORC1 in vitro in primary neurons and in vivo in the developing cerebral cortex of the mouse. Of note, reduced expression of these genes upon mTORC1 inhibition translated into reduced cholesterol levels. We further show that while mTORC1 does not regulate chromatin accessibility or RNA stability of these genes it drives transcription of their DNA. Using a bioinformatics approach, we identified binding sites for the transcription factors SREBP, SP1 and NF-Y to be enriched in the promoters of mTORC1 target genes and confirmed binding of NF-YA by ChIP-qPCR. Altogether, our results indicate that mTORC1 is an important regulator of the expression of sterol/cholesterol biosynthesis genes in the developing brain. Altered expression of these genes may be an important contributing factor in the pathogenesis of neurodevelopmental disorders associated with dysregulated mTOR signaling.

Introduction

Although changes in the activity of the mTOR pathway are associated with numerous neurodevelopmental disorders the molecular basis of disease development remains poorly understood. The mTOR pathway is a central signaling pathway in the cell that controls gene expression at multiple levels. While mTOR is most famous for its role in regulating translation of specific target mRNAs it in addition regulates RNA stability and gene transcription [1-7]. In proliferating cells such as fibroblasts and cancer cells,

mTORC1 controls transcription of glycolytic, lipid and lysosome biogenesis and mitochondrial metabolism genes [1, 3]. It activates several transcription factors involved in metabolic processes including sterol regulatory element binding proteins (SREBPs) and hypoxia inducible factor-1α (HIF1α) [1, 8-10].

Most likely, dysregulation of transcriptional processes contributes to disease development in neurodevelopmental disorders that are associated with changes in mTOR activity – yet mTOR mediated transcriptional regulation in the brain is heavily understudied.

In the brain, the mTOR signaling pathway controls various different processes such as neuronal differentiation, neuronal cell size, axon guidance, dendritogenesis and synaptic plasticity [11]. Dysregulation of the mTOR pathway is associated with neurodevelopmental disorders including epilepsy, autism spectrum disorder (ASD) and intellectual disability (ID). In this context, both hyper- and hypoactive mTOR signaling are connected to disease. While mTOR hyperactivity was observed in disorders such as fragile X syndrome (FXS), neurofibromatosis 1 (NF1) and tuberous sclerosis mTOR hypoactivity was characteristic of a mouse model of Rett syndrome and of human embryonic stem cell (hESC) derived neurons that carried a *MECP2* loss-of-function allele [12-16]. In addition, hemizygous germline mutations in the X chromosomal *MID1* gene lead to decreased mTOR signaling and Opitz BBB/G syndrome, a midline malformation disorder and ID syndrome [17].

The evolutionary conserved mTOR kinase comprises the core of two protein complexes, mTOR complex 1 (mTORC1) and 2 (mTORC2) [18]. mTOR activity is regulated intracellularly by nutrients, energy level and stress factors (e.g. hypoxia) and extracellularly by growth factors (e.g. brain derived neurotrophic factor (BDNF)), hormones (e.g. insulin), neurotransmitters and cytokines. Upon activation mTORC1 phosphorylates eukaryotic translation initiation factor 4E (eIF4E) binding proteins (4E-BP1 and 4E-BP2) and S6 kinases (S6K1 and S6K2). Both phosphorylation of the 4E-BPs and S6Ks comprise critical steps in the initiation of cap-dependent translation. For instance, phosphorylation of the 4E-BPs leads to their inactivation and dissociation from 5'cap bound EIF4E whereas phosphorylation of the S6Ks leads to their activation. S6Ks in turn phosphorylate proteins (e.g. ribosomal protein S6) that control different steps of translation [18]. Two studies showed that mTOR inhibition in fibroblasts and prostate cancer cells has a moderate effect on the translation of most mRNAs. It, however,

strongly downregulated translation of a subgroup of mRNAs, many of which involved in protein synthesis, that contained specific sequence motifs, the 5′-terminal oligopyrimidine tract (5'TOP) or a pyrimidine-rich translational element (PRTE), in their 5'-untranslated regions (5'UTRs) [19, 20].

While translation regulation by mTOR has been studied extensively in the brain, much less is known about mTOR mediated transcriptional regulation.

Here we used 3'mRNA sequencing (3'mRNA-Seq) to identify mTOR dependent genes in neurons treated with the mTOR inhibitor temsirolimus. We found that temsirolimus treatment downregulated expression of numerous genes of the sterol/cholesterol biosynthesis pathway resulting in decreased cholesterol levels.

Injection of rapamycin into pregnant dams confirmed our results *in vivo* in the developing cerebral cortex. While we did not find changes in RNA stability or chromatin accessibility, we identified binding sites for the transcription factors SP1, SREBP and NF-Y that were enriched in the promoter regions of the downregulated genes. ChIP-qPCR analyses confirmed binding of NF-YA to mTOR target gene promoters. Interestingly, NF-YA binding to these promoters increased in temsirolimus treated neurons. Our findings strongly suggest an important role for the mTOR pathway in regulating the expression of metabolic genes in neurons and in the developing brain.

Methods

Mice, cell culture and drug treatment

NMRI (8-12 weeks old) mice were ordered from Janvier labs (Saint Berthevin, France) and sacrificed by cervical dislocation. For neuron culture primary cortical neurons were isolated from E14.5 embryos from pregnant NMRI mice. After collection of brains, cortices were dissected out and mechanically separated into single cells via resuspension. The neurons were plated on Poly-L-Ornithine (Sigma, St. Louis, USA)- and Laminin (Sigma)-coated plates and cultured in Neurobasal medium (Gibco, Carlsbad, USA), supplemented with 2% B-27 plus vitamin A (Gibco) and 1% GlutaMAX (Gibco), in a humidified incubator at 37 °C and 8 % CO2. For drug treatment, primary cortical neurons were cultured for 6 days in 6-well-plates followed by treatment with the mTOR inhibitor temsirolimus (10 μM; Sigma, St. Louis, USA) diluted in culture medium for 5 or 24 hours. For measuring RNA stability, neurons were treated with the transcriptional

blocker Actinomycin D (Sigma, St. Louis, USA; 5 µg/ml). For further analyses, cells were harvested in PBS using cell scrapers. For in vivo experiments 8-12 weeks old pregnant NMRI mice received a single intraperitoneal (i. p.) injection at stage E16.5 or were injected i. p. once daily with rapamycin (LC Laboratories, Woburn, USA) or DMSO (control vehicle) on three consecutive days (E14.5-16.5). A single injection contained either 10 µl DMSO or 10 µl rapamycin (1 mg/kg) dissolved in 100 % DMSO. Twenty-four hours after the last injection, embryonic cortices were isolated and stored either in Lysis Buffer (48% Urea, 14 mM Tris pH 7,5, 8,7% Glycerol, 1% SDS, Protease inhibitor cocktail) or RNAlater for further analysis at –80 °C.

Immunoblotting:

Antibodies for immunoblotting were as follows: phospho-S6, S6 (Cell Signaling Technology, Danvers, USA), Osc, Mvd (Santa Cruz Biotechnology, Santa Cruz, USA), Ldlr, Nsdhl (Novus Biologicals, Centennial, USA), GAPDH (Abcam, Cambridge, UK). Western blot analysis was performed by standard methods using enhanced chemiluminescence.

RNA Isolation, cDNA synthesis, RT-qPCR and RNA sequencing:

The total RNA extraction with TRIzol reagent from brain tissue was performed as recommended by Invitrogen Life Technologies (Carlsbad, USA). High Pure RNA Isolation Kit (Roche, Basel, CH) was used to extract total RNA from cell samples using spin columns. The purity, quantity, and integrity of the RNA were measured with a NanoDrop One spectrophotometer. The cDNA samples were synthesized from 500 to 1000 ng total RNA using the PrimeScriptTM RT Master Mix cDNA (Takara, Kyoto, JAP) according to the manufacturer's instructions. Quantitative real-time PCR (qRT-PCR) was carried out using SYBR® Premix Ex Taq™ II (Tli RNaseH Plus) and 10 µM primers (final concentration), according to the manufacturer's instructions. RT-qPCR reactions were performed on an ABI StepOnePlus Real-Time PCR System using intron spanning primers with the following conditions: 95 °C/30 s, 40 cycles of 95 °C/5 s, 60 °C/30 s, 72 °C/30 s. For primer sequences see Supplementary table S1. All reactions were measured in triplicates, and median cycles to threshold (Ct) values were used for analysis. The housekeeping gene GAPDH was used for normalization, and relative gene expression was determined using the $2^{-\Delta\Delta CT}$ method.

For RNA sequencing, RNA purity and integrity were measured using the Agilent 2100 bioanalyzer (Agilent Technologies, Santa Clara, USA). RNA was converted into cDNA by

using QuantSeq 3′mRNA-Seq Reverse (REV) Library Prep Kit (Lexogen, Vienna, AU) according to manufacturer's instruction to generate compatible library (2.5 pM) for Illumina sequencing. RNA sequencing was performed using a high output reagent cartridge v2 (75 cycles; Illumina, San Diego, USA) with a custom primer (0.3 μM) provided by Lexogen on an Illumina NextSeq 500 device.

RNA-Seq data analysis

After the sequencing bcl2fastq v2.17.1.14 conversion software (Illumina, Inc.) was used to demultiplex sequence data and convert base call (BCL) files into Fastq files. Sequencing adapters (AGATCGGAAGAG) were trimmed and reads shorter than 6 nucleotides were removed from further analysis using Cutadapt v1.11 [21]. Quality control checks were performed on the trimmed data with FastQC v0.11.4 [22]. Read mapping of the trimmed data against the mouse reference genome and transcriptome (mm9) were conducted using STAR aligner v2.5.3 [23]. To estimate the expression levels of each transcript the mapped reads were assigned to annotated features using the Subread tool featureCounts v1.5.2 [24]. The output of the raw read counts from featureCounts were used as an input for the differential expression analysis using the combination of DESeq2 v1.16.1 [25] and edgeR v3.26.8 [26] packages. Pairwise comparison analysis of two different conditions was carried out with edgeR to normalized the expression levels of known genes and only genes with CPM (counts per million) > 10 were further analyzed. The differentially expressed gene analysis was performed on the normalized genes expression using DESeq2 with |log2FoldChange| > 0.5 and padj (adjusted p-value) > 0.05.

Chromatin Immunoprecipitation (ChIP)-qPCR:

DMSO or temsirolimus treated cells were pelleted and resuspended in cold PBS and later fixed with 1% formaldehyde in PBS for 10 min at room temperature, followed by quenching with 125 mM glycine for 5 min. Fixed cells were resuspended in 140 mM RIPA (10 mM Tris-Cl pH 8.0, 140 mM NaCl, 0.1 mM EDTA pH 8.0, 1% Triton X-100, and 0.1% SDS) and subjected to 20 cycles of sonication using Bioruptor Pico (Diagenode, Liège, BEL), with 30 secs “ON”/ “OFF” at high settings. After sonication, samples were centrifuged at 14,000 × g for 10 min at 4 °C and supernatant was transferred to a fresh tube. Input material was collected at this stage (4% of input). The extracts were

incubated overnight with 1 µg (1:500 dilution) of NF-YA (Santa Cruz) and IgG control (Santa Cruz) antibodies at 4 °C with head-over tail rotations. After overnight incubations, 20 µl of blocked Protein A and G Dynabeads (Diagenode) were added to the tubes and further incubated for 3 h to capture the antibodies. Bead separation was carried out using a magnetic rack and washed as following; once with 140 mM RIPA (10 mM Tris-Cl pH 8.0, 140 mM NaCl, 0.1 mM EDTA pH 8.0, 1% Triton X-100, and 0.1% SDS), four times with 250 mM RIPA (10 mM Tris-Cl pH 8.0, 250 mM NaCl, 0.1 mM EDTA pH 8.0, 1% Triton X100, and 0.1% SDS) and twice with TE buffer pH 8.0 (10 mM Tris-Cl pH 8.0 and 0.1 mM EDTA pH 8.0). For reversal of cross-linking, samples were RNase-treated (NEB) and subjected to Proteinase K treatment for 12 h at 37 °C and at least 6 h at 65 °C after the immunoprecipitation. After proteinase K treatment, the DNA was extracted using the phenol-chloroform method. After precipitating and pelleting, DNA was dissolved in 20 µl of TE buffer. The input and chromatin immunoprecipitated material were processed identically across the samples. The fluorescent signal of the amplified DNA was normalized to input.

ATAC-seq:

ATAC-seq was done as previously described (Buenrostro et al., 2013). Briefly, 50,000 DMSO or temsirolimus treated cell were resuspended in cold lysis buffer (10 mM Tris-HCl, pH 7.4, 10 mM NaCl, 3 mM $MgCl_2$ and 0.1% IGEPAL CA-630) and centrifuged at 750g for 30 min using a refrigerated centrifuge. Immediately following the cell prep, the pellet was resuspended in the transposase reaction mix (25 µL 2× TD buffer, 2.5 µL transposase (Illumina, San Diego, USA) and 22.5 µL nuclease-free water). The transposition reaction was carried out for 30 min at 37 °C. Following transposition, the sample was purified using a Qiagen MinElute kit. Following purification, library was amplified using 1× NEBnext PCR master mix and 1.25 µM of custom Nextera PCR primers 1 and 2 (Buenrostro et al. 2013), using the following PCR conditions: 72 °C for 5 min; 98 °C for 30 s; and thermocycling at 98 °C for 10 s, 63 °C for 30 s and 72 °C for 1 min. After 11–12 cycles of PCR amplification, sample was further purified using Qiagen MinElute kit. To remove primer dimer samples were further purified using AMPure beads XP (Beckman Coulter, Brea, USA) with a ratio of x0.9 of beads to samples. Samples were then analyzed in bioanalyzer (Agilent Technologies) and sequenced on an Illumina NextSeq 500.

ATAC-seq data analysis:

ATAC-Seq data quality check was performed using reads FASTQC v0.11.8 [22]. Further, adaptors were removed using Trimmomatic v0.39 [27]. Paired-end ATAC-Seq reads were mapped to Mus musculus genome (mm10) UCSC annotations using Bowtie2 v2.3.5.1 [28] with default parameters. Properly paired end reads with high mapping quality (MAPQ ≥10) were retained in analysis with help of Samtools v1.7 [29]. Next, using Picard tools MarkDuplicates [30] utility duplicates were removed. ATAC-Seq peaks were called using MACS2 v2.1.1.20160309 [31]. ATAC peaks were visualized with USCS genome browser [32].

Cholesterol Assay:

Primary cortical neurons were treated with DMSO or temsirolimus at days in vitro (DIV) 4 for 48 hours and with Cyclodextrin (Sigma, St. Louis, USA) for one hour before cholesterol measurement. The AmplexTM Red Cholesterol Assay (Thermo Fisher Scientific, Waltham, USA) was performed in a 96 well plate by the reaction of 50 µL of Amplex Red working solution with 50 µL of assay sample. 5 ml of working solution, prepared prior to the analysis, contained 75 µL of a 300 µM of Amplex Red reagent and 2 U/mL of HRP, 2 U/ml cholesterol oxidase and 0,2 U/ml cholesterol esterase. The working solution volume was adjusted to 5 mL with reaction buffer, which contained 25 mM potassium phosphate, pH 7.4, 12.5 mM NaCl, 1.25 mM cholic acid and 0.025 % TritonX-100. The reactions were incubated for 30 min at 37°C, protected from light. After incubation, fluorescence was measured in a fluorescence microplate reader FLUOstar Optima (BMG Labtech, Ortenberg, GER) using excitation wavelength at 560 nm and emission detection at 590 nm.

Statistical analyses

All statistical analyses except for NGS analyses were done with GraphPad Prism 5 or Microsoft Office Excel. Data are shown as mean + standard error of the mean. Statistical analyses were done using Student's *t*-test. p values < 0.05 were considered statistically significant.

Gene ontology analysis and KEGG pathway analysis:

For differentially up- and down-regulated expressed genes of each pairwise comparison as well as overlapping genes for SREBP, NFY and SP1 motifs, an over representation analysis (ORA) was carried out with clusterProfiler v3.4.4 [33]. All expressed genes within the pairwise comparison samples with CPM > 10 served as a background for the analysis. The Bioconductor org.Mm.eg.db v 3.8.2 mouse annotation package [34] and mouse KEGG.db [35] was used for the gene ontology analysis and KEGG analysis, respectively. The default parameters were used for all over-representation tests.

Motif identification

Motif discovery analysis was performed using HOMER (Hypergeometric Optimization of Motif EnRichment) Software v4.9 [36]. ATAC-Seq sequencing data from 186 genes in FASTA format served as input for the findMotif.pl function. Scrambled of input sequences (randomized) was created automatically by HOMER and used as a background for the motif analysis.

Results

Transcriptional targets downstream of mTOR in neurons

To identify mTOR dependent transcriptional changes we treated primary cortical neurons with the mTOR inhibitor temsirolimus for 5 h or 24 h. Temsirolimus treatment caused strong downregulation in mTOR activity as measured by the ratio of the mTOR downstream effector pS6/S6 (Figure 1A) and carried out 3'mRNA-Seq. We identified a total of 522 differentially expressed genes (DEGs) at 5 h and 1090 DEGs at 24 h of temsirolimus treatment with an overlap of 241 DEGs between the two time points (0.5 log2Fold change and adjusted p-val <0.05). Of all DEGs 315 and 564 were upregulated at 5 and 24 h, respectively and 207 and 526 were downregulated (Figure 1 B and C, Supplementary table S2).

Because mTOR is best known for its function in gene activation, we decided to focus on the set of genes downregulated upon mTOR inhibition in subsequent analyses. Several studies have reported mTOR regulated transcriptional changes in non-neuronal cells. For instance Duvel et al. used Tsc1-/- and Tsc2-/- fibroblasts, which exhibit growth factor independent activation of mTORC1, in combination with rapamycin treatment. The authors found that mTORC1 activates expression of numerous genes involved in

glycolysis, pentose phosphate pathway and lipin/sterol biosynthesis. We used the dataset published by Duvel et al. to identify mTOR-dependent transcriptional changes shared between fibroblasts and neurons. Surprisingly, when we compared our set of downregulated genes with the 130 genes found to be upregulated by mTORC1 in fibroblasts only 13 genes overlapped between both sets after 5 h of temsirolimus treatment and only 20 genes after 24 h (Figure 1 D, Supplementary table S2).

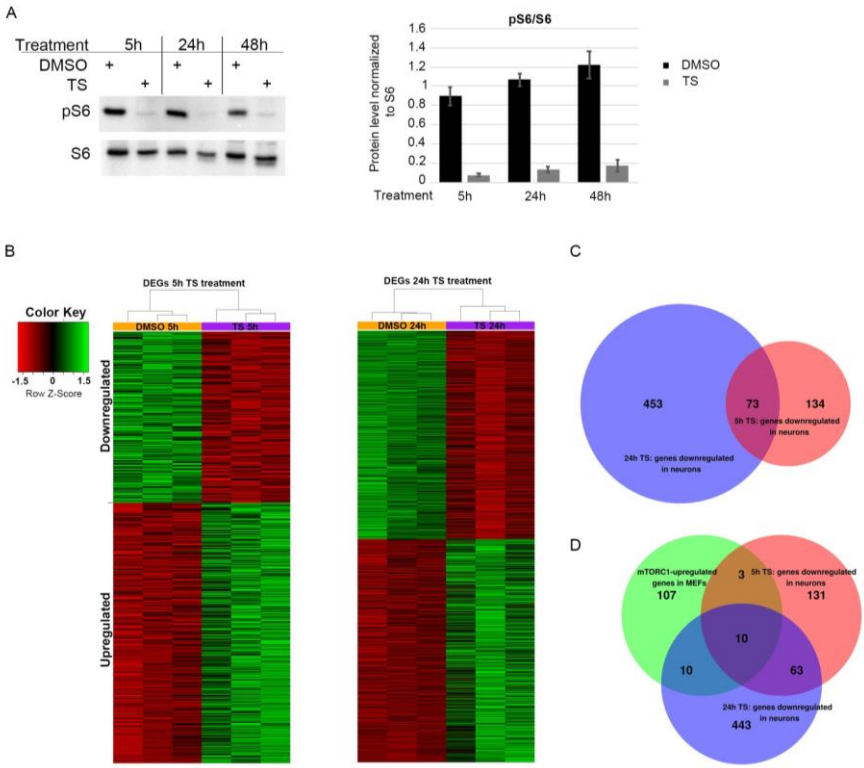

Fig 1: Temsirolimus treatment leads to widespread gene expression changes in primary neurons.
Primary cortical neurons at DIV6 were treated with temsirolimus (10 µM) or vehicle (DMSO) for 5, 24 or 48 hours and subjected to western blot analysis (A) or RNA-Seq (B-C). (A) The cells were lysed at the indicated time points and subjected to immunoblot analysis with pS6 and S6 specific antibodies. Bands were quantified using ChemiDoc software. (B-D) For RNA-Seq analysis total RNA was extracted from DMSO and temsirolimus treated neurons and converted into cDNA using QuantSeq 3′mRNA-Seq Reverse (REV) Library Prep Kit. (B) Heat maps indicating genes differentially expressed (DEGs) between neurons treated with DMSO or temsirolimus for 5 or 24 hours. (C) Venn diagram of genes downregulated after 5 or 24 hours of temsirolimus treatment. (D) Venn diagram showing the overlap between genes downregulated in neurons after 5 and 24 hours of temsirolimus treatment and upregulated in mTOR hyperactive mouse embryonic fibroblasts (MEFs)

mTOR regulates expression of genes of the cholesterol pathway in primary neurons

Gene ontology analysis revealed that genes downregulated after 5 or 24 h of temsirolimus treatment were enriched for metabolic terms (Figure 2A). These terms comprised sterol/lipid biosynthesis/metabolism processes including the cholesterol

biosynthesis pathway (Figure 2A). Other metabolic pathways previously described to be dependent on mTOR signaling like glycolysis and pentose phosphate pathway were, however, not enriched. By directly analyzing gene expression changes from our RNA-seq data we could confirm a general downregulation of sterol/cholesterol pathway genes. Genes of the glycolysis pathway, however, remained unaltered in their expression (Figure 2B). Also, by RT-qPCR several genes of the cholesterol biosynthesis process showed a 40 – 60% downregulation after 5 h of temsirolimus treatment (Figure 2 C). Westernblot experiments confirmed a significant downregulation of two of the three tested genes at protein level after 24 h of temsirolimus treatment (Figure 2 D). In contrast to genes of the cholesterol biosynthesis pathway, genes of the glycolysis pathway (Pfkp, Pgm2 and Pdk1) remained unaltered in their expression (Figure 2C). Temsirolimus is a derivative of rapamycin, a binder of FK506-binding protein-12 (FKBP-12) and allosteric partial inhibitor of the mTORC1 kinase. In contrast to rapamycin (and temsirolimus) ATP-competitive inhibitors like Torin 1 inhibit the phosphorylation of all mTORC1 substrates. The observed effect that temsirolimus treatment caused inhibition of the genes of some but not all metabolic pathways previously described to be dependent on mTOR activity could theoretically be due to temsirolimus being a partial mTORC1 inhibitor. In a next step we therefore treated neurons with Torin 1 for 5 h. Similar to temsirolimus treatment the cholesterol biosynthesis pathway genes Ldlr and Dhcr7 were significantly downregulated after 5 h of Torin 1 treatment (Supplementary figure S1). In addition and in contrast to temsirolimus treatment, however, the glycolysis pathway genes Pfkp, Pgm2 and Pdk1 were also significantly downregulated (Supplementary figure S1).

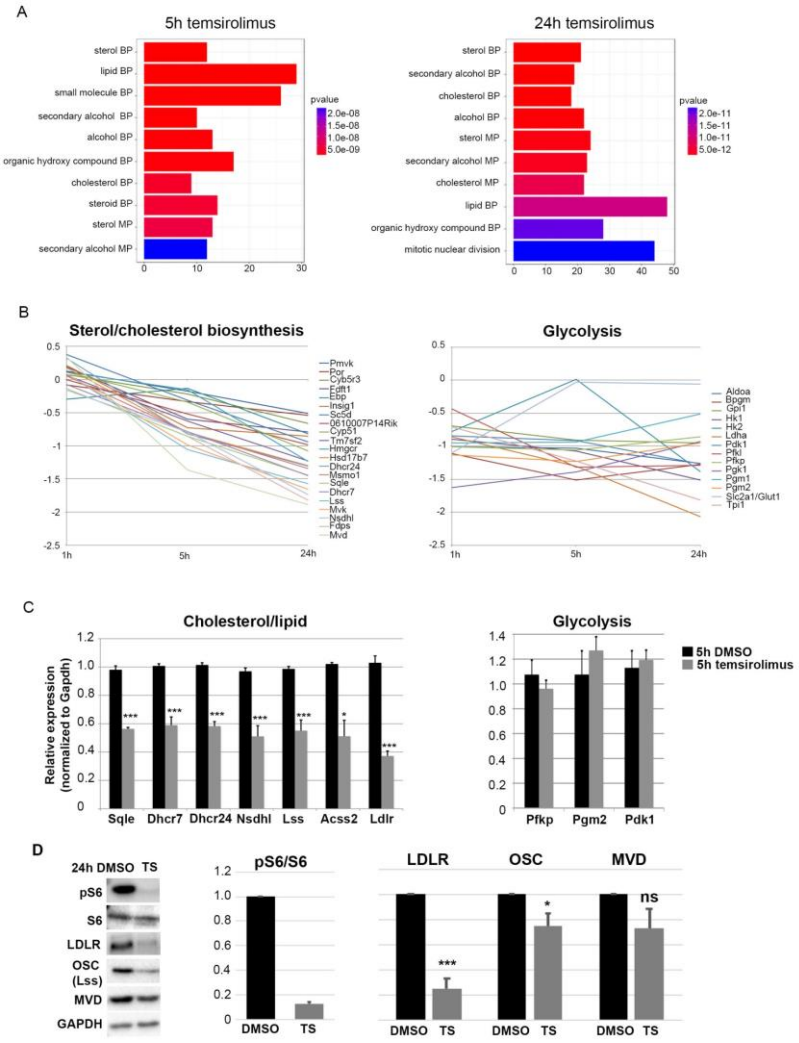

Fig 2: Temsirolimus treatment causes downregulation of genes of the cholesterol biosynthesis pathway.
(A) Barplots of top 10 GO enriched terms of downregulated genes after 5 hours (left) and 24 hours (right) of temsirolimus treatment. Both plots show a high enrichment for metabolic pathways shown on the y-axis and the number of gene count on the x-axis. Enrichment scores are depicted in the colored bar. (B) Inhibition of mTORC1 by temsirolimus treatment downregulates genes of the sterol and cholesterol biosynthesis pathway but does not change expression of glycolysis genes. (C) Confirmation of changes in the expression of cholesterol/glycolysis genes by RT-qPCR. Cells were lysed after 5 hours of temsirolimus/DMSO treatment and subjected to total RNA extraction and RT-qPCR; mRNA expression was normalized to Gapdh. (D) Western blot experiments in primary neurons after treatment with DMSO or temsirolimus for 24 hours. Reduction in pS6 in relation to S6 confirms mTORC1 inhibition. Expression pattern of proteins involved in cholesterol biosynthesis. Data represent the average of three biological replicates. For statistical analyses, student's t test was used.

mTOR activity is essential for proper expression of cholesterol pathway genes in the embryonic cerebral cortex

Having shown that mTOR promotes expression of cholesterol pathway genes in primary neurons *in vitro* we next wanted to verify this type of regulation in the brain *in vivo*. While neurons of the adult brain rely mainly on astrocytes for cholesterol providing a

critical time window during prenatal development exists where neuronal cholesterol synthesis is essential for neurons to differentiate normally [37]. To analyze if mTOR activity is required for the expression of cholesterol pathway genes we therefore chose to inhibit mTOR prenatally, starting at E16.5 by injecting rapamycin which has the same mechanism of action as temsirolimus intraperitoneally into pregnant mice. Twenty-four hours after a single dose of rapamycin injection we observed a strong inhibition of the mTOR pathway as shown by westernblot analysis of the mTOR downstream effector pS6 (Figure 3A). Already at this time point all four tested cholesterol pathway genes (Ldlr, Osc, Mvd, Dhcr7) were reduced in their mRNA expression by about 50% (Figure 3B). In contrast, only Ldlr was significantly reduced by about 20% at protein level at this time point (Figure 3C). Because the low effect on protein level could possibly be due to enhanced protein stability we, in a next step injected rapamycin on three consecutive days. Surprisingly, after 3 days of injection mRNA levels of the four genes tested had returned back to their normal levels which might be due to compensatory effects (Figure 3D). Protein expression of Ldlr, Mvd and Nsdhl was, however, significantly reduced by 45, 30 and 25%, respectively (Figure 3E).

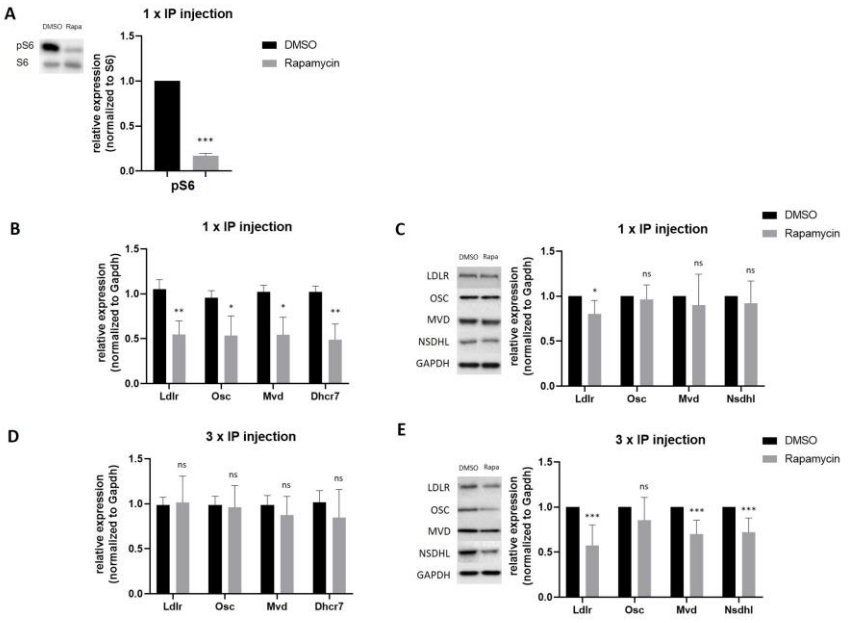

Fig 3: mTORC1 inhibition in the embryonic cerebral cortex downregulates cholesterol biosynthesis genes in vivo.
Pregnant mice received either a single injection at E16.5 or were injected on three following days (E14.5-E16.5) once per day with DMSO or rapamycin at a dose of 1 mg/kg. Subsequently, total RNA and protein was extracted from the cerebral cortex and RT-qPCR and western blot experiments were performed. (A) Inhibition of mTORC1 activity was confirmed by western blot anaylsis of the mTORC1 downstream effector pS6 (in comparison to S6) 24 hours after a single injection of rapamycin. (B,D) RT-qPCR to detect RNA expression of the four genes Ldlr, Osc, Mvd and Dhcr7 after a one-day (B) or three-days (D) i. p. injection of rapamycin compared to DMSO; mRNA expression was normalized to Gapdh. (C,E) Immunoblot analysis to detect LDLR, OSC, MVD and DHCR7 protein expression after a one-day (B) or three-days (D) i. p. injection of rapamycin compared to DMSO and normalized to Gapdh. Data represent the average of six biological replicates. For statistical analyses, student's t test was used. *P < 0.05; **P < 0.01; ***P < 0.001.

Reduced cholesterol production in mTOR inhibited neurons

After 5 and 24 h of temsirolimus treatment eight and fifteen genes of the cholesterol biosynthesis pathway, respectively, were significantly downregulated in their expression (Figure 4A, Supplementary figure S2). The cholesterol biosynthesis pathway can be separated into three sections according to the type of compounds which are produced - mevalonate, isoprenoids and sterols. After 24 h of temsirolimus treatment genes of all three sections were downregulated in their expression, including the gene encoding HMGCR which catalyzes the rate limiting step in cholesterol biosynthesis, the reduction of HMG-CoA to mevalonate.

We therefore expected impaired cholesterol biosynthesis in neurons treated with temsirolimus. To test for this, we treated cortical neurons with temsirolimus for two days and performed Amplex Red cholesterol assays. When compared with DMSO treated neurons, cholesterol levels were significantly downregulated in temsirolimus treated neurons as well as in neurons treated with cyclodextrin, a cholesterol depleting reagent which served as positive control (Figure 4B).

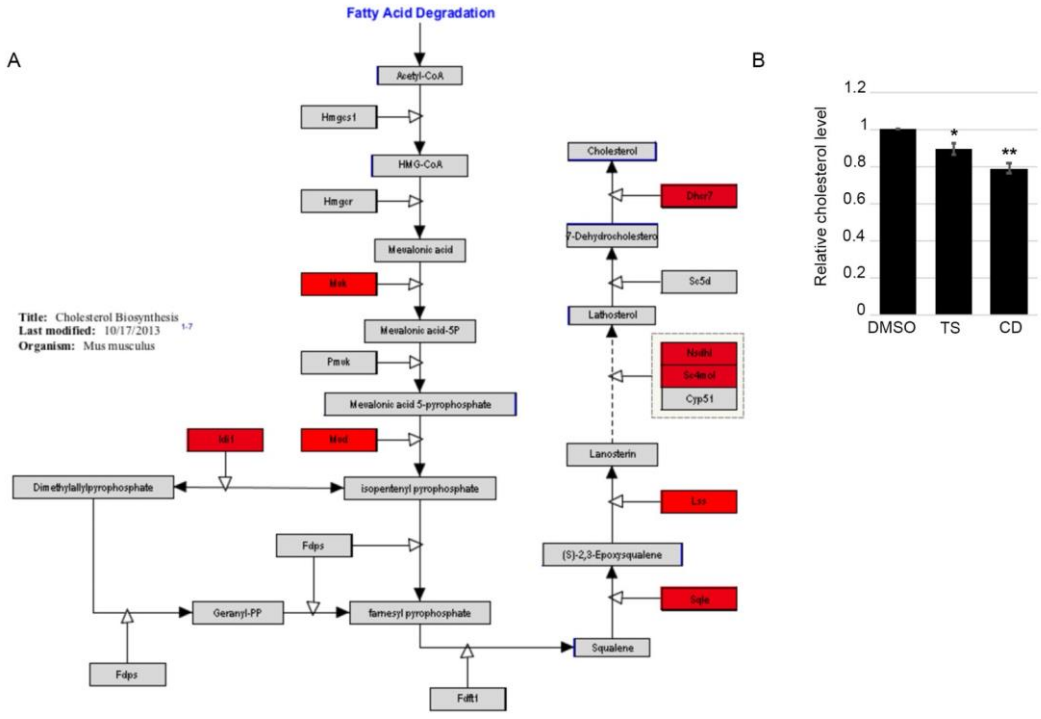

Fig 4: Temsirolimus treatment of reduces cholesterol levels in primary neurons.
(A) Schematic overview of the cholesterol synthesis pathway in the mouse. Genes identified as being downregulated in the RNA-Seq experiment after temsirolimus treatment are marked in red. (B) Changes in cholesterol levels were identified in DIV 6 primary cortical neurons treated with DMSO, temsirolimus (both for 48 hours) or cyclodextrin (for one hour) using Amplex Red Cholesterol Assay Kit.

mTOR dependent genes contain SREBP, NF-YA and SP1 binding sites in their promoter regions

mRNA expression changes can be mediated at the epigenetic level, by changes in chromatin accessibility, at the transcriptional level, by changes in transcription factor binding or at the posttranscriptional level, by changes in mRNA stability. It was demonstrated before that mTOR activation can both enhance transcription of metabolic genes and increase their mRNA stability [1, 6]. To test for possible mRNA stability changes we treated primary neurons with the transcriptional inhibitor Actinomycin D in combination with temsirolimus or DMSO and measured the mRNA decay rate of three of the downregulated targets, Ldlr, Osc and Nsdhl. None of the three mRNAs underwent a decrease in its stability upon mTOR inhibition which suggests that posttranscriptional regulation of mRNA expression is not a general mechanism of gene regulation under these experimental conditions (Supplementary figure S3A-C).

To test for mTOR mediated changes in chromatin accessibility, in a next step we employed an assay for Transposase-Accessible Chromatin with high-throughput sequencing (ATAC-seq) on biological replicates (n=2 for each condition) from cortical neurons treated with temsirolimus or DMSO. We identified 62,225 and 53,051 (Replicate 1); 119,339 and 90,435 (Replicate 2) open chromatin regions in DMSO and temsirolimus treated neurons, respectively ($P<0.05$; Supplementary Table S3). The majority of open chromatin regions mapped to promoters, introns and intergenic regions of annotated genes (Supplementary figure S3D). When comparing open chromatin regions of DMSO and temsirolimus neurons we could, however, not identify major differences, especially not in those regions associated with genes involved in cholesterol biosynthesis (Supplementary figure S3E). This suggests that modifications in chromatin accessibility do not play a major role in mediating gene expression changes after temsirolimus treatment. Rather, this suggests that mTOR mediated activation of gene expression in neurons occurs directly at the level of transcription factor regulation.

Düvel and colleagues showed that, in MEFs, the binding site for SREBPs is over-represented in the promoters of mTOR regulated targets. When using the software findM [38] to screen the promoter regions of the genes downregulated in neurons treated with temsirolimus for 5 h we found that 44.9% of them contained at least one such binding site (Fig. 5A).

In a next step we applied the software Homer [36] on 5h Ts vs DMSO downregulated genes to identify additional transcription factor binding sites in an unbiased manner.

This analysis revealed that the binding sites for the transcription factors SP1 and NF-Y, respectively, occurred in 76.3 and 31.4 % of the promoters of the downregulated genes. SREBPs, which are weak transcriptional activators on their own, cooperate with other transcription factors on their target promoters. Two key interaction partners of SREBP1 are SP1 and NF-Y [39]. In our data we found that of the 93 downregulated genes that contained an SREBP binding motif in their promoters 83 (89.2%) also contained an SP1 motif and 38 (40.9%) an NF-Y motif. Interestingly, the majority (36 out of 38) of downregulated genes that contained both an SREBP and an NF-Y binding site additionally contained an SP1 motif in their promoters.

Identification of enriched GO terms revealed that genes involved in the sterol/cholesterol biosynthesis pathway preferentially contained binding sites for all three (SREBP, NF-Y, SP1) or two (NF-Y, SP1) of the three factors or in their promoters. In non-neuronal cells, mTORC1 regulates nuclear abundance of SREBP1; the SREBP transcription factors are required for mTOR induced expression of metabolic genes [1, 8]. Much less is, however, known about the connection between mTOR activity and NF-Y functioning. The NF-Y complex is a trimer and consists of NF-YA, NF-YB and NF-YC. Having histone-like structures, NF-YB and NF-YC, upon hetero-dimerization build a platform for NF-YA to associate. NF-YA then provides sequence specific motif recognition. Although most studies report a function for NF-YA as transcriptional activator a repressor function has been described as well [40-42]. Inspection of our RNA-seq data revealed no change in gene expression of either NF-YA, NF-YB or NF-YC 5h or 24h after temsirolimus treatment. Also, NF-YA predominantly localized to the nucleus under all experimental conditions and thus its subcellular localization did not change in temsirolimus treated neurons as determined by immunofluorescence analysis (Supplementary Figure S4). To test for changes in NF-Y binding after mTOR inhibition and because NF-YA is responsible for directing the NF-Y complex to its target sequences, we treated primary neurons with DMSO or temsirolimus and performed ChIP-qPCR with NF-YA specific antibodies. Since NF-Y mainly acts as a transcriptional activator we expected to see a decrease in NF-YA binding to its target sites within the promoters of mTOR regulated genes upon mTOR inhibition. Surprisingly, however, we observed the opposite. NF-Y showed an increased binding to the promoter of the known target Aurka as well as to the promoters of the mTOR target genes Mvd and Nsdhl upon mTOR inhibition.

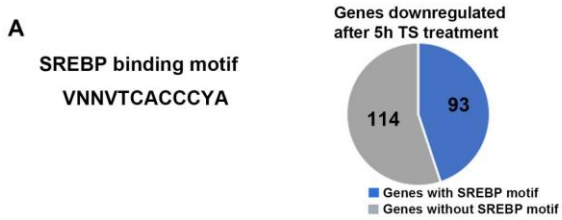

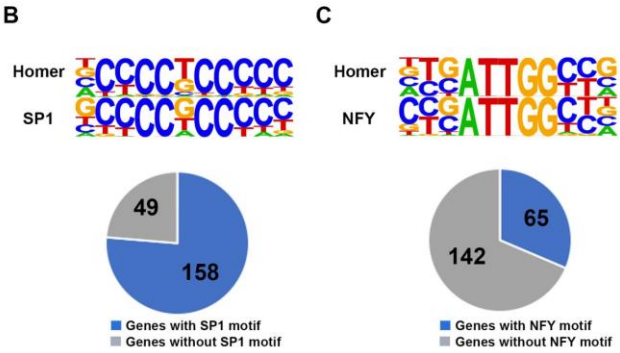

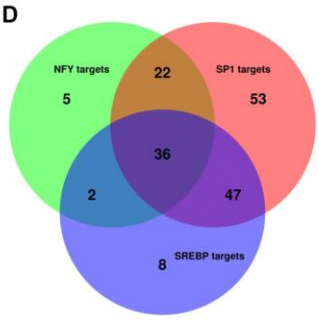

E

Transcription factor	GO term	Number of genes	p Value (adjusted)
SREBP, NFY, SP1 (n = 35)	Sterol biosynthesis	5	5.13×10^{-5}
	Lipid biosynthesis	9	0.0002
	Cholesterol biosynthesis	3	0.006
NFY, SP1 (n = 22)	Sterol biosynthesis	4	0.0003
	Cholesterol biosynthesis	3	0.002
SREBP, SP1 (n = 48)	-		
SREBP (n = 7) NFY (n = 5) SP1 (n = 53)	- - -		

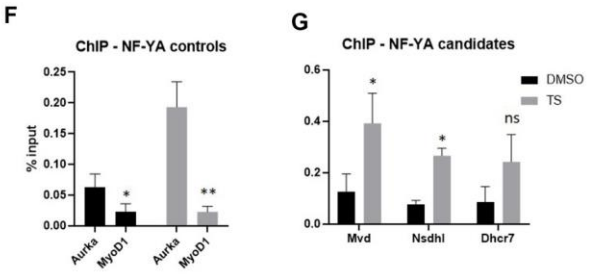

Fig 5: Analysis of transcription factor binding in mTORC1 inhibited neurons.
(A) Venn diagram of the genes downregulated after temsirolimus treatment which contain SREBP binding sites in their promoters. For SREBP binding site identification, the software findM was used. (B,C) Venn diagrams of the genes which were downregulated after temsirolimus treatment and contain SP1 (B) or NF-Y (C) binding sites their promoters. The software Homer was used to screen the promoters of the downregulated genes for the presence of transcription factor binding sites. (D) Venn diagram depicting downregulated genes which share binding sites for two or three of the transcription factors SREBP, SP1 and NF-Y in their promoters. (E) GO term analysis of the genes which contain different combinations of transcription factor binding sites in their promoters. (F,G) ChIP was performed with NF-YA specific antibodies in neurons treated for 5 hours with DMSO or temsirolimus followed by qPCR of positive control Aurka and negative control MyoD (F) or the downregulated targets Mvd, Nsdhl and Dhcr7 (G). Data represent the average of three biological replicates. For statistical analyses, student's t test was used. *P < 0.05; **P < 0.01; ***P < 0.001.

Discussion

By the use of several non-neuronal cellular systems such as fibroblasts, regulatory T cells and cancer cell lines it was shown previously that the mTOR kinase is an important transcriptional activator of metabolic genes [1, 3, 5]. It has not yet been investigated whether mTOR also controls the transcription of metabolic genes in neuronal cells in the brain - although mTOR signaling is an essential pathway for brain development and mTOR dysregulation causes a variety of neurodevelopmental disorders. Therefore, dysregulation of metabolic gene expression may very likely contribute to neurological symptoms in mTOR associated disorders. Here we show that mTOR drives the expression of metabolic genes of the sterol/cholesterol pathway in primary cortical neurons in vitro and in the developing cerebral cortex in vivo.

Although in neurons like in non-neuronal cells mTOR promotes expression of metabolic genes we observed some major differences between the different cell types. In neurons treated with temsirolimus we observed downregulation of genes of the cholesterol biosynthesis pathway but not of the glycolysis and pentose phosphate pathway which were both affected in mTOR hyperactive fibroblasts treated with rapamycin [1]. One explanation for this discrepancy might be the different experimental conditions. Indeed, when we treated cortical neurons with the more potent mTOR inhibitor, Torin 1, which inhibits the phosphorylation of all mTORC1 substrates we not only observed gene downregulation in the cholesterol biosynthesis pathway but also in the glycolysis pathway. In addition, prior studies suggest that cell type-specific effects exist which are likely to contribute to the differences observed between non-neuronal cell types and neurons. Thus depending on the cell type, mTOR activates specific transcription factors such as HIF1α, SREBPs and TFEB in fibroblasts and IRF4 and GATA3 in regulatory T cells [1, 3, 43]. Even nuclear localization and DNA binding of mTOR itself was observed [5, 9, 44]. Which mechanisms contribute to regulating cholesterol gene expression by mTOR in neurons is still unclear. We found a significant enrichment of binding sites for the transcription factors SP1, SREBPs and NF-Y in the promoters of mTOR regulated genes in neurons. ChIP analyses confirmed the binding of NF-YA to all investigated promoters. Of note NF-YA binding was increased upon mTOR inhibition. As a member of the NF-Y complex, which also contains NF-YB and NF-YC, NF-YA mediates DNA binding specificity to the CCAAT motif in the proximal promoter region [45]. NF-Y regulates an increasing number of genes and is ubiquitously expressed, so it's likely to have different roles depending on the context. The NF-YA knockout in mice causes early embryonic lethality

[46]. In proliferating cells such as embryonic fibroblasts and hematopoietic stem cells, NF-Y is involved in cell cycle regulation [47-50]. While it is often downregulated during differentiation [51, 52] NF-Y is active in mature neurons of the adult mouse brain where its deletion causes neurodegeneration [53, 54]. NF-Y co-localizes with other transcription factors such as FOS at genomic sites [55]. In differentiating neurons and HEK293 cells it was found that NF-YA and JNK bind to the same genomic sites and that NF-YA recruits JNK to these sites [56]. In addition, it was shown that NF-Y interacts at target gene promoters in cooperation with SREBP1 or SREBP2 and SP1 and activates genes of metabolic pathways [39, 57, 58]. The fact that NF-YA binding at mTOR responsive promoters increased after mTOR inhibition suggests a mechanism where NF-YA may be important to recruit other transcription factors, such as SREBPs to mTOR responsive promoters. In the case of mTOR downregulation a hypothetic feedback mechanism might act to increase binding of NF-YA to these promoters.

Downregulation of mTOR activity is thought to play an important role in the pathogenesis of neurodevelopmental disorders such as Rett syndrome and CDKL5 deficiency disorder [13, 59, 60]. How reduced mTOR activity contributes to disease development in these disorders is, however, not entirely clear. Defects in the cholesterol pathway may be one contributing mechanism. Even small perturbations in cholesterol metabolism can largely affect neuronal development [61-64]. Low levels of cholesterol have been associated with a variety of neurodevelopmental disorders. Cholesterol biosynthesis is a multistep process which is divided into a pre- and post-squalene pathway (Fig. 3A). Several genes of the cholesterol biosynthesis pathway are mutated in neurodevelopmental syndromes. The most common genetic syndrome associated with defects in cholesterol biosynthesis is the autosomal recessive Smith Lemli Opitz syndrome (SLOS; OMIM# 270400) which is caused by mutations in *DHCR7* encoding the enzyme 7-dehydrocholesterol D7reductase. The neurological symptoms of SLOS include epilepsy, intellectual disability and behavioural problems, among others. Mutations in *NSDHL* are associated with the X-linked dominant disorder CHILD syndrome (OMIM #308050) and the X-linked recessive disorder CK syndrome (OMIM #300831), mutations in *MVK* with the autosomal recessive disorder Mevalonic Aciduria (OMIM #610377). All three syndromes are characterized by structural brain abnormalities and/or neurological symptoms including intellectual disability. The gene product of *NSDHL*, 3β-hydroxysteroid dehydrogenase is involved in one of the later steps in

cholesterol biosynthesis, the gene product of *MVK*, mevalonate kinase, is a peroxisomal enzyme involved in cholesterol biosynthesis in the pre-squalene pathway. Of note expression of all three genes, *Dhcr7*, *Nsdhl* and *Mvk* was downregulated in temsirolimus treated neurons (Fig. 2B). Although these results suggest that perturbations in cholesterol biosynthesis in disorders associated with mTOR downregulation may contribute to disease development several things have to be addressed in future studies. Thus, it is still unclear whether mTOR downregulation leads to long lasting defects in cholesterol biosynthesis and reduced cholesterol levels. In the *in vivo* experiments we observed that 24h after injecting a single dose of rapamycin the mRNA expression of all tested genes was decreased. After three days of rapamycin injection expression, however, had returned to normal levels (Fig. 4A, B). This observation hints to the existence of feedback or compensatory mechanisms. Indeed, cholesterol biosynthesis involves several feedback mechanisms [65]. Buchovecky and colleagues found that in the brains of a mouse model for Rett syndrome (*Mecp2* null mice) total cholesterol was increased at P56 when mutant males have severe symptoms. At a later age (P70), however, brain cholesterol levels were comparable to wildtype levels which reflected reduced cholesterol synthesis. Likely, the over production of cholesterol had fed back to later decrease cholesterol synthesis. Of note genetic or pharmacologic inhibition of cholesterol synthesis ameliorated some of the symptoms in these mice.

Our studies were limited to mTOR mediated regulation of cholesterol biosynthesis in cortical neurons. While the brain needs to synthesize its own cholesterol even during development when the blood brain barrier has not fully formed yet, neuronal cholesterol synthesis is most important during a critical developmental time window [37]. Neurons in the adult brain rely mainly on astrocytes for providing cholesterol. In addition, during myelination oligodendrocytes synthesize huge amounts of cholesterol. It was already shown in zebrafish that cholesterol is needed for mTOR activity in oligodendrocyte precursor cells and that mTOR regulates cholesterol-dependent myelin gene expression [66]. An open question therefore is whether mTOR signaling in astrocytes and oligodendrocytes is equally important for cholesterol biosynthesis as it is in neurons.

Acknowledgements

Martin Schüle was supported by stipends from the Focus Program of Translational Neurosciences of the Johannes Gutenberg-University Mainz. This work was supported by the Deutsche Forschungsgemeinschaft (CRC 1193).

Authors' contribution

MS designed and performed experiments, analyzed the data and wrote the manuscript, TB designed and performed experiments and analyzed the data. SS, SG and KE designed experiments and analyzed the data. SD analyzed the data. JW planned experiments, analyzed the data and wrote the manuscript. All authors read and approved the final manuscript.

Conflict of interest statement

The authors declare no competing financial interests.

References

1. Duvel K, Yecies JL, Menon S, Raman P, Lipovsky AI, Souza AL, et al. Activation of a metabolic gene regulatory network downstream of mTOR complex 1. Mol Cell. 2010;39(2):171-83. Epub 2010/07/31. doi: 10.1016/j.molcel.2010.06.022. PubMed PMID: 20670887; PubMed Central PMCID: PMCPMC2946786.
2. Avet-Rochex A, Carvajal N, Christoforou CP, Yeung K, Maierbrugger KT, Hobbs C, et al. Unkempt is negatively regulated by mTOR and uncouples neuronal differentiation from growth control. PLoS Genet. 2014;10(9):e1004624. Epub 2014/09/12. doi: 10.1371/journal.pgen.1004624. PubMed PMID: 25210733; PubMed Central PMCID: PMCPMC4161320.
3. Chapman NM, Zeng H, Nguyen TM, Wang Y, Vogel P, Dhungana Y, et al. mTOR coordinates transcriptional programs and mitochondrial metabolism of activated Treg subsets to protect tissue homeostasis. Nat Commun. 2018;9(1):2095. Epub 2018/05/31. doi: 10.1038/s41467-018-04392-5. PubMed PMID: 29844370; PubMed Central PMCID: PMCPMC5974344.
4. Guertin DA, Guntur KV, Bell GW, Thoreen CC, Sabatini DM. Functional genomics identifies TOR-regulated genes that control growth and division. Curr Biol. 2006;16(10):958-70. Epub 2006/05/23. doi: 10.1016/j.cub.2006.03.084. PubMed PMID: 16713952.
5. Audet-Walsh E, Dufour CR, Yee T, Zouanat FZ, Yan M, Kalloghlian G, et al. Nuclear mTOR acts as a transcriptional integrator of the androgen signaling pathway in prostate cancer. Genes Dev. 2017. Epub 2017/07/21. doi: 10.1101/gad.299958.117. PubMed PMID: 28724614; PubMed Central PMCID: PMCPMC5558925.
6. Lee G, Zheng Y, Cho S, Jang C, England C, Dempsey JM, et al. Post-transcriptional Regulation of De Novo Lipogenesis by mTORC1-S6K1-SRPK2 Signaling. Cell. 2017;171(7):1545-58 e18. Epub 2017/11/21. doi: 10.1016/j.cell.2017.10.037. PubMed PMID: 29153836; PubMed Central PMCID: PMCPMC5920692.

7. Peng T, Golub TR, Sabatini DM. The immunosuppressant rapamycin mimics a starvation-like signal distinct from amino acid and glucose deprivation. Mol Cell Biol. 2002;22(15):5575-84. Epub 2002/07/09. doi: 10.1128/mcb.22.15.5575-5584.2002. PubMed PMID: 12101249; PubMed Central PMCID: PMCPMC133939.
8. Peterson TR, Sengupta SS, Harris TE, Carmack AE, Kang SA, Balderas E, et al. mTOR complex 1 regulates lipin 1 localization to control the SREBP pathway. Cell. 2011;146(3):408-20. Epub 2011/08/06. doi: 10.1016/j.cell.2011.06.034. PubMed PMID: 21816276; PubMed Central PMCID: PMCPMC3336367.
9. Bernardi R, Guernah I, Jin D, Grisendi S, Alimonti A, Teruya-Feldstein J, et al. PML inhibits HIF-1alpha translation and neoangiogenesis through repression of mTOR. Nature. 2006;442(7104):779-85. Epub 2006/08/18. doi: 10.1038/nature05029. PubMed PMID: 16915281.
10. Kelsey I, Zbinden M, Byles V, Torrence M, Manning BD. mTORC1 suppresses PIM3 expression via miR-33 encoded by the SREBP loci. Sci Rep. 2017;7(1):16112. Epub 2017/11/25. doi: 10.1038/s41598-017-16398-y. PubMed PMID: 29170467; PubMed Central PMCID: PMCPMC5701013.
11. Garza-Lombo C, Gonsebatt ME. Mammalian Target of Rapamycin: Its Role in Early Neural Development and in Adult and Aged Brain Function. Front Cell Neurosci. 2016;10:157. Epub 2016/07/06. doi: 10.3389/fncel.2016.00157. PubMed PMID: 27378854; PubMed Central PMCID: PMCPMC4910040.
12. Lee DY. Roles of mTOR Signaling in Brain Development. Exp Neurobiol. 2015;24(3):177-85. Epub 2015/09/29. doi: 10.5607/en.2015.24.3.177. PubMed PMID: 26412966; PubMed Central PMCID: PMCPMC4580744.
13. Li Y, Wang H, Muffat J, Cheng AW, Orlando DA, Loven J, et al. Global transcriptional and translational repression in human-embryonic-stem-cell-derived Rett syndrome neurons. Cell Stem Cell. 2013;13(4):446-58. Epub 2013/10/08. doi: S1934-5909(13)00401-3 [pii]
10.1016/j.stem.2013.09.001. PubMed PMID: 24094325.
14. Ricciardi S, Boggio EM, Grosso S, Lonetti G, Forlani G, Stefanelli G, et al. Reduced AKT/mTOR signaling and protein synthesis dysregulation in a Rett syndrome animal model. Hum Mol Genet. 2011;20(6):1182-96. Epub 2011/01/08. doi: ddq563 [pii] 10.1093/hmg/ddq563. PubMed PMID: 21212100.
15. Hoeffer CA, Sanchez E, Hagerman RJ, Mu Y, Nguyen DV, Wong H, et al. Altered mTOR signaling and enhanced CYFIP2 expression levels in subjects with fragile X syndrome. Genes Brain Behav. 2012;11(3):332-41. Epub 2012/01/25. doi: 10.1111/j.1601-183X.2012.00768.x. PubMed PMID: 22268788; PubMed Central PMCID: PMCPMC3319643.
16. Sharma A, Hoeffer CA, Takayasu Y, Miyawaki T, McBride SM, Klann E, et al. Dysregulation of mTOR signaling in fragile X syndrome. J Neurosci. 2010;30(2):694-702. Epub 2010/01/15. doi: 10.1523/JNEUROSCI.3696-09.2010. PubMed PMID: 20071534; PubMed Central PMCID: PMCPMC3665010.
17. Liu E, Knutzen CA, Krauss S, Schweiger S, Chiang GG. Control of mTORC1 signaling by the Opitz syndrome protein MID1. Proc Natl Acad Sci U S A. 2011;108(21):8680-5.
18. Switon K, Kotulska K, Janusz-Kaminska A, Zmorzynska J, Jaworski J. Molecular neurobiology of mTOR. Neuroscience. 2017;341:112-53. Epub 2016/11/28. doi: 10.1016/j.neuroscience.2016.11.017. PubMed PMID: 27889578.
19. Thoreen CC, Chantranupong L, Keys HR, Wang T, Gray NS, Sabatini DM. A unifying model for mTORC1-mediated regulation of mRNA translation. Nature. 2012;485(7396):109-13. Epub 2012/05/04. doi: 10.1038/nature11083. PubMed PMID: 22552098; PubMed Central PMCID: PMCPMC3347774.

20. Hsieh AC, Liu Y, Edlind MP, Ingolia NT, Janes MR, Sher A, et al. The translational landscape of mTOR signalling steers cancer initiation and metastasis. Nature. 2012;485(7396):55-61. Epub 2012/03/01. doi: 10.1038/nature10912. PubMed PMID: 22367541; PubMed Central PMCID: PMCPMC3663483.
21. Martin M. Cutadapt removes adapter sequences from high-throughput sequencing reads. EMBnetjournal. 2011;17(1). doi: https://doi.org/10.14806/ej.17.1.200.
22. Andrew S. FastQC: a quality control tool for high throughput sequence data. Available online at: http://wwwbioinformaticsbabrahamacuk/projects/fastqc. 2010.
23. Dobin A, Davis CA, Schlesinger F, Drenkow J, Zaleski C, Jha S, et al. STAR: ultrafast universal RNA-seq aligner. Bioinformatics. 2013;29(1):15-21. Epub 2012/10/30. doi: 10.1093/bioinformatics/bts635. PubMed PMID: 23104886; PubMed Central PMCID: PMCPMC3530905.
24. Liao Y, Smyth GK, Shi W. featureCounts: an efficient general purpose program for assigning sequence reads to genomic features. Bioinformatics. 2014;30(7):923-30. Epub 2013/11/15. doi: 10.1093/bioinformatics/btt656. PubMed PMID: 24227677.
25. Love MI, Huber W, Anders S. Moderated estimation of fold change and dispersion for RNA-seq data with DESeq2. Genome Biol. 2014;15(12):550. Epub 2014/12/18. doi: 10.1186/s13059-014-0550-8. PubMed PMID: 25516281; PubMed Central PMCID: PMCPMC4302049.
26. Robinson MD, McCarthy DJ, Smyth GK. edgeR: a Bioconductor package for differential expression analysis of digital gene expression data. Bioinformatics. 2010;26(1):139-40. Epub 2009/11/17. doi: 10.1093/bioinformatics/btp616. PubMed PMID: 19910308; PubMed Central PMCID: PMCPMC2796818.
27. Bolger AM, Lohse M, Usadel B. Trimmomatic: a flexible trimmer for Illumina sequence data. Bioinformatics. 2014;30(15):2114-20. Epub 2014/04/04. doi: 10.1093/bioinformatics/btu170. PubMed PMID: 24695404; PubMed Central PMCID: PMCPMC4103590.
28. Langmead B, Salzberg SL. Fast gapped-read alignment with Bowtie 2. Nat Methods. 2012;9(4):357-9. Epub 2012/03/06. doi: 10.1038/nmeth.1923. PubMed PMID: 22388286; PubMed Central PMCID: PMCPMC3322381.
29. Li H, Handsaker B, Wysoker A, Fennell T, Ruan J, Homer N, et al. The Sequence Alignment/Map format and SAMtools. Bioinformatics. 2009;25(16):2078-9. Epub 2009/06/10. doi: 10.1093/bioinformatics/btp352. PubMed PMID: 19505943; PubMed Central PMCID: PMCPMC2723002.
30. Broad institute GR. Picard Toolkit. http://broadinstitutegithubio/picard/;Broad Institute. 2019.
31. Zhang Y, Liu T, Meyer CA, Eeckhoute J, Johnson DS, Bernstein BE, et al. Model-based analysis of ChIP-Seq (MACS). Genome Biol. 2008;9(9):R137. Epub 2008/09/19. doi: 10.1186/gb-2008-9-9-r137. PubMed PMID: 18798982; PubMed Central PMCID: PMCPMC2592715.
32. Kent WJ, Sugnet CW, Furey TS, Roskin KM, Pringle TH, Zahler AM, et al. The human genome browser at UCSC. Genome Res. 2002;12(6):996-1006. Epub 2002/06/05. doi: 10.1101/gr.229102. PubMed PMID: 12045153; PubMed Central PMCID: PMCPMC186604.
33. Yu G, Wang LG, Han Y, He QY. clusterProfiler: an R package for comparing biological themes among gene clusters. OMICS. 2012;16(5):284-7. Epub 2012/03/30. doi: 10.1089/omi.2011.0118. PubMed PMID: 22455463; PubMed Central PMCID: PMCPMC3339379.

34. Carlson M. org.Mm.eg.db: Genome wide annotation for Mouse. R package version 3.8.2. 2019.
35. Kanehisa M, Sato Y, Kawashima M, Furumichi M, Tanabe M. KEGG as a reference resource for gene and protein annotation. Nucleic Acids Res. 2016;44(D1):D457-62. Epub 2015/10/18. doi: 10.1093/nar/gkv1070. PubMed PMID: 26476454; PubMed Central PMCID: PMCPMC4702792.
36. Heinz S, Benner C, Spann N, Bertolino E, Lin YC, Laslo P, et al. Simple combinations of lineage-determining transcription factors prime cis-regulatory elements required for macrophage and B cell identities. Mol Cell. 2010;38(4):576-89. Epub 2010/06/02. doi: 10.1016/j.molcel.2010.05.004. PubMed PMID: 20513432; PubMed Central PMCID: PMCPMC2898526.
37. Funfschilling U, Jockusch WJ, Sivakumar N, Mobius W, Corthals K, Li S, et al. Critical time window of neuronal cholesterol synthesis during neurite outgrowth. J Neurosci. 2012;32(22):7632-45. Epub 2012/06/01. doi: 10.1523/JNEUROSCI.1352-11.2012. PubMed PMID: 22649242; PubMed Central PMCID: PMCPMC6703588.
38. Ambrosini G, Praz V, Jagannathan V, Bucher P. Signal search analysis server. Nucleic Acids Res. 2003;31(13):3618-20. Epub 2003/06/26. doi: 10.1093/nar/gkg611. PubMed PMID: 12824379; PubMed Central PMCID: PMCPMC169017.
39. Reed BD, Charos AE, Szekely AM, Weissman SM, Snyder M. Genome-wide occupancy of SREBP1 and its partners NFY and SP1 reveals novel functional roles and combinatorial regulation of distinct classes of genes. PLoS Genet. 2008;4(7):e1000133. Epub 2008/07/26. doi: 10.1371/journal.pgen.1000133. PubMed PMID: 18654640; PubMed Central PMCID: PMCPMC2478640.
40. Nassiri M, Liu J, Kulak S, Uwiera RR, Aird WC, Ballermann BJ, et al. Repressors NFI and NFY participate in organ-specific regulation of von Willebrand factor promoter activity in transgenic mice. Arterioscler Thromb Vasc Biol. 2010;30(7):1423-9. Epub 2010/05/01. doi: 10.1161/ATVBAHA.110.206680. PubMed PMID: 20431063; PubMed Central PMCID: PMCPMC3653838.
41. Peng Y, Jahroudi N. The NFY transcription factor functions as a repressor and activator of the von Willebrand factor promoter. Blood. 2002;99(7):2408-17. Epub 2002/03/16. doi: 10.1182/blood.v99.7.2408. PubMed PMID: 11895773.
42. Li G, Zhao H, Wang L, Wang Y, Guo X, Xu B. The animal nuclear factor Y: an enigmatic and important heterotrimeric transcription factor. Am J Cancer Res. 2018;8(7):1106-25. Epub 2018/08/11. PubMed PMID: 30094088; PubMed Central PMCID: PMCPMC6079162.
43. Pena-Llopis S, Vega-Rubin-de-Celis S, Schwartz JC, Wolff NC, Tran TA, Zou L, et al. Regulation of TFEB and V-ATPases by mTORC1. EMBO J. 2011;30(16):3242-58. Epub 2011/08/02. doi: 10.1038/emboj.2011.257. PubMed PMID: 21804531; PubMed Central PMCID: PMCPMC3160667.
44. Rosner M, Hengstschlager M. Cytoplasmic and nuclear distribution of the protein complexes mTORC1 and mTORC2: rapamycin triggers dephosphorylation and delocalization of the mTORC2 components rictor and sin1. Hum Mol Genet. 2008;17(19):2934-48. Epub 2008/07/11. doi: 10.1093/hmg/ddn192. PubMed PMID: 18614546.
45. Maity SN, de Crombrugghe B. Role of the CCAAT-binding protein CBF/NF-Y in transcription. Trends Biochem Sci. 1998;23(5):174-8. Epub 1998/06/05. doi: 10.1016/s0968-0004(98)01201-8. PubMed PMID: 9612081.
46. Bhattacharya A, Deng JM, Zhang Z, Behringer R, de Crombrugghe B, Maity SN. The B subunit of the CCAAT box binding transcription factor complex (CBF/NF-Y) is

essential for early mouse development and cell proliferation. Cancer Res. 2003;63(23):8167-72. Epub 2003/12/18. PubMed PMID: 14678971.
47. Gurtner A, Fuschi P, Magi F, Colussi C, Gaetano C, Dobbelstein M, et al. NF-Y dependent epigenetic modifications discriminate between proliferating and postmitotic tissue. PLoS One. 2008;3(4):e2047. Epub 2008/04/24. doi: 10.1371/journal.pone.0002047. PubMed PMID: 18431504; PubMed Central PMCID: PMCPMC2295263.
48. Benatti P, Dolfini D, Vigano A, Ravo M, Weisz A, Imbriano C. Specific inhibition of NF-Y subunits triggers different cell proliferation defects. Nucleic Acids Res. 2011;39(13):5356-68. Epub 2011/03/19. doi: 10.1093/nar/gkr128. PubMed PMID: 21415014; PubMed Central PMCID: PMCPMC3141247.
49. Di Agostino S, Strano S, Emiliozzi V, Zerbini V, Mottolese M, Sacchi A, et al. Gain of function of mutant p53: the mutant p53/NF-Y protein complex reveals an aberrant transcriptional mechanism of cell cycle regulation. Cancer Cell. 2006;10(3):191-202. Epub 2006/09/09. doi: 10.1016/j.ccr.2006.08.013. PubMed PMID: 16959611.
50. Imbriano C, Gnesutta N, Mantovani R. The NF-Y/p53 liaison: well beyond repression. Biochim Biophys Acta. 2012;1825(2):131-9. Epub 2011/12/06. doi: 10.1016/j.bbcan.2011.11.001. PubMed PMID: 22138487.
51. Gurtner A, Manni I, Fuschi P, Mantovani R, Guadagni F, Sacchi A, et al. Requirement for down-regulation of the CCAAT-binding activity of the NF-Y transcription factor during skeletal muscle differentiation. Mol Biol Cell. 2003;14(7):2706-15. Epub 2003/07/15. doi: 10.1091/mbc.e02-09-0600. PubMed PMID: 12857858; PubMed Central PMCID: PMCPMC165670.
52. Farina A, Manni I, Fontemaggi G, Tiainen M, Cenciarelli C, Bellorini M, et al. Down-regulation of cyclin B1 gene transcription in terminally differentiated skeletal muscle cells is associated with loss of functional CCAAT-binding NF-Y complex. Oncogene. 1999;18(18):2818-27. Epub 1999/06/11. doi: 10.1038/sj.onc.1202472. PubMed PMID: 10362252.
53. Yamanaka T, Miyazaki H, Oyama F, Kurosawa M, Washizu C, Doi H, et al. Mutant Huntingtin reduces HSP70 expression through the sequestration of NF-Y transcription factor. EMBO J. 2008;27(6):827-39. Epub 2008/02/22. doi: 10.1038/emboj.2008.23. PubMed PMID: 18288205; PubMed Central PMCID: PMCPMC2274932.
54. Yamanaka T, Tosaki A, Kurosawa M, Matsumoto G, Koike M, Uchiyama Y, et al. NF-Y inactivation causes atypical neurodegeneration characterized by ubiquitin and p62 accumulation and endoplasmic reticulum disorganization. Nat Commun. 2014;5:3354. Epub 2014/02/26. doi: 10.1038/ncomms4354. PubMed PMID: 24566496.
55. Fleming JD, Pavesi G, Benatti P, Imbriano C, Mantovani R, Struhl K. NF-Y coassociates with FOS at promoters, enhancers, repetitive elements, and inactive chromatin regions, and is stereo-positioned with growth-controlling transcription factors. Genome Res. 2013;23(8):1195-209. Epub 2013/04/19. doi: 10.1101/gr.148080.112. PubMed PMID: 23595228; PubMed Central PMCID: PMCPMC3730095.
56. Tiwari VK, Stadler MB, Wirbelauer C, Paro R, Schubeler D, Beisel C. A chromatin-modifying function of JNK during stem cell differentiation. Nat Genet. 2011;44(1):94-100. Epub 2011/12/20. doi: 10.1038/ng.1036. PubMed PMID: 22179133.
57. Benatti P, Chiaramonte ML, Lorenzo M, Hartley JA, Hochhauser D, Gnesutta N, et al. NF-Y activates genes of metabolic pathways altered in cancer cells. Oncotarget. 2016;7(2):1633-50. Epub 2015/12/10. doi: 10.18632/oncotarget.6453. PubMed PMID: 26646448; PubMed Central PMCID: PMCPMC4811486.

58. Schiavoni G, Bennati AM, Castelli M, Della Fazia MA, Beccari T, Servillo G, et al. Activation of TM7SF2 promoter by SREBP-2 depends on a new sterol regulatory element, a GC-box, and an inverted CCAAT-box. Biochim Biophys Acta. 2010;1801(5):587-92. Epub 2010/02/09. doi: 10.1016/j.bbalip.2010.01.013. PubMed PMID: 20138239.
59. Della Sala G, Putignano E, Chelini G, Melani R, Calcagno E, Michele Ratto G, et al. Dendritic Spine Instability in a Mouse Model of CDKL5 Disorder Is Rescued by Insulin-like Growth Factor 1. Biol Psychiatry. 2016;80(4):302-11. Epub 2015/10/11. doi: 10.1016/j.biopsych.2015.08.028. PubMed PMID: 26452614.
60. Wang IT, Allen M, Goffin D, Zhu X, Fairless AH, Brodkin ES, et al. Loss of CDKL5 disrupts kinome profile and event-related potentials leading to autistic-like phenotypes in mice. Proc Natl Acad Sci U S A. 2012;109(52):21516-21. Epub 2012/12/14. doi: 10.1073/pnas.1216988110. PubMed PMID: 23236174; PubMed Central PMCID: PMCPMC3535652.
61. Keber R, Motaln H, Wagner KD, Debeljak N, Rassoulzadegan M, Acimovic J, et al. Mouse knockout of the cholesterogenic cytochrome P450 lanosterol 14alpha-demethylase (Cyp51) resembles Antley-Bixler syndrome. J Biol Chem. 2011;286(33):29086-97. Epub 2011/06/28. doi: 10.1074/jbc.M111.253245. PubMed PMID: 21705796; PubMed Central PMCID: PMCPMC3190716.
62. Waterham HR. Defects of cholesterol biosynthesis. FEBS Lett. 2006;580(23):5442-9. Epub 2006/08/01. doi: 10.1016/j.febslet.2006.07.027. PubMed PMID: 16876788.
63. Zhang J, Liu Q. Cholesterol metabolism and homeostasis in the brain. Protein Cell. 2015;6(4):254-64. Epub 2015/02/16. doi: 10.1007/s13238-014-0131-3. PubMed PMID: 25682154; PubMed Central PMCID: PMCPMC4383754.
64. Driver AM, Kratz LE, Kelley RI, Stottmann RW. Altered cholesterol biosynthesis causes precocious neurogenesis in the developing mouse forebrain. Neurobiol Dis. 2016;91:69-82. Epub 2016/02/28. doi: 10.1016/j.nbd.2016.02.017. PubMed PMID: 26921468; PubMed Central PMCID: PMCPMC4860088.
65. Ahmad F, Sun Q, Patel D, Stommel JM. Cholesterol Metabolism: A Potential Therapeutic Target in Glioblastoma. Cancers (Basel). 2019;11(2). Epub 2019/01/30. doi: 10.3390/cancers11020146. PubMed PMID: 30691162; PubMed Central PMCID: PMCPMC6406281.
66. Mathews ES, Appel B. Cholesterol Biosynthesis Supports Myelin Gene Expression and Axon Ensheathment through Modulation of P13K/Akt/mTor Signaling. J Neurosci. 2016;36(29):7628-39. Epub 2016/07/23. doi: 10.1523/JNEUROSCI.0726-16.2016. PubMed PMID: 27445141; PubMed Central PMCID: PMCPMC4951573.